

# GLOBAL SIMULATION OF THE LiCAS/RTRS SURVEY SYSTEM FOR THE ILC

G. Grzelak\*, University of Warsaw, Poland

P. Brockill, S. Cohen, J. Dale, Y. Han, M. Jones, G. Moss, A. Reichold,  
C. Uribe-Estrada, R. Wastie, S. Yang, University of Oxford and JAI, United Kingdom  
J. Prenting, M. Schlösser, DESY, Hamburg, Germany

## Abstract

The LiCAS<sup>1</sup> metrology system installed inside the Rapid Tunnel Reference Surveyor (RTRS) is a novel instrument designed to the survey of reference network in the International Linear Collider (ILC) linac tunnel. Two modern measurement techniques: Laser Straightness Monitors (LSM) and Frequency Scanning Interferometry (FSI) for absolute distance measurement [1, 2] will deliver an accuracy beyond conventional open air optical metrology. Detailed simulations of the LiCAS RTRS surveying a long accelerator tunnel have been performed. Error propagation study for the reference wall markers co-ordinates are presented for statistical and systematic errors. We demonstrate that the LiCAS instrument is capable to survey the ILC tunnel to the desired accuracy of  $O(200) \mu m$  in vertical direction over 600 m tunnel section.

## PRINCIPLE OF THE LICAS-RTRS TRAIN OPERATION

The first prototype of the LiCAS train operating in DESY test tunnel is composed of 3 cars with the distance between the centres of neighbouring cars equal to 4.5 m. However, basing on the results of the propagation of systematic uncertainties presented in this paper we decided to change the base line design of the train. The proposed configuration consists of 4 cars with the car to car separation of 25 m. All results presented in this paper refer to such a train operating over 600 m tunnel section (24 train stops) which corresponds to the betatron wave length of the ILC.

Technical details of the LiCAS-RTRS train were introduced in separate presentations [3, 4, 5]. In figure 1 the sensing parts of the LiCAS cars are presented. Each car is equipped with 4 CCD cameras and two beam splitters (BS) constituting the straightness monitor. The straightness monitor measures the transverse translation ( $T_x, T_y$ ) and transverse rotation ( $R_x, R_y$ ) with respect to a  $z$  axis defined by the laser beam passing through all cars in a vacuum pipe. The laser beam is reflected back using the retro-reflector (RR) located in the last car, illuminating the upper CCD cameras of the straightness monitors. 6 internal FSI lines placed in the same vacuum pipe between each pair of cars are responsible for the distance measurement along the  $z$  axis ( $T_z$ ). In addition a clinometer located on

each car provides a measurement of rotation around the  $z$  axis ( $R_z$ ). 6 external FSI lines pointing towards the accelerator wall determine the position of the reference markers. The redundancy existing in all subcomponents allows to reduce measurements errors and also makes possible to preserve the functionality of the entire system in case of hardware failures. It can be also used to cross-check selected measurements against each other during calibration phase. In figure 2 the schematic view of the LiCAS train operating in the accelerator tunnel was shown. When the train stops in front of the wall markers it firstly measures the relative position and rotation of all cars with respect to the first car. This defines the local reference frame of the train in which the location of the wall mounted reference markers are measured next. This procedure is repeated for each train stop. Each marker is measured up to 4 times. Finally the coordinates of each marker, expressed in the local train frames are transformed to the frame of the first train (the global frame) by fitting them to each other under the constraint that wall markers have not moved during the entire measurement.

## SOFTWARE USED IN THE ANALYSIS

In order to model the LiCAS train operating inside the accelerator tunnel and to study the expected performance of this device a detailed numerical simulation has been performed. It consists of the description of the geometry of the system, ray tracer emulating the actual measurements, position reconstruction and error propagation package used for the estimation of statistical errors. In addition LiCAS train Monte Carlo was developed to study the effect of accumulating systematic errors.

### *Definition of the Geometry and Ray Tracer*

This part of the package is responsible for preparing input for further calculations by generating positions and angles of active objects inside the LiCAS train: CCD cameras, Beam Splitters (BS) and laser beam for straightness monitor, internal and external FSI lines for distance measurements (INTFSI, EXTFSI) including light sources and retro-reflectors. The tunnel wall is also populated by equidistant wall markers. For each sensing object its nominal co-ordinates are defined together with the “deltas” – small random distortion to make the model more realistic allowing for non-trivial calibration constants.

\* grzelak@fuw.edu.pl

<sup>1</sup>Linear Collider Alignment and Survey R&D group

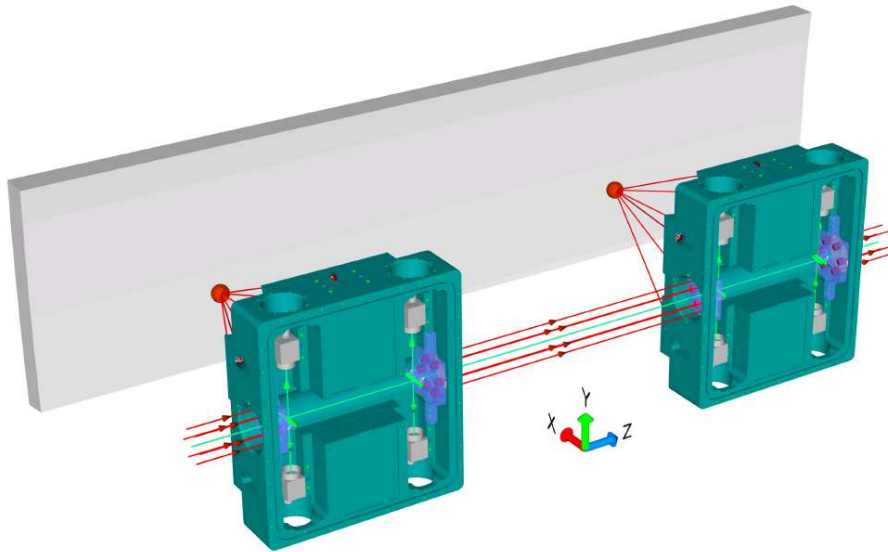


Figure 1: Mechanical design of the measurement units for the LiCAS train. The sensing parts of each car are composed of 4 CCD cameras and 2 beam splitters (BS) constituting the straightness monitor and 6 internal FSI lines to measure the distance between the cars. The 6 external FSI lines pointing towards the tunnel wall measure the position of wall markers. In addition each car is equipped with a clinometer (not shown).

The positions and rotation matrixes of various objects are subsequently transformed from local car frames to higher level frames of each train and the global tunnel frame. An additional randomisation at this stage is also possible accounting for the arbitrary position and orientation of the cars at particular train stops.

Having defined the positions and angles of all participating objects the actual measurements are simulated using the straight line ray tracing (light scattering off the beam splitters and CCD measurements) as well as the distance measurements of the FSI lines. The measurements are smeared by the resolution of the corresponding sensors.

### Reconstruction and Error Propagation

In order to study the expected precision on the position reconstruction of the tunnel reference markers the SIMULGEO [6] package was used which allows for modelling of the opto-geometrical systems. This programme can be used in two different modes: (i) reconstruction and (ii) error propagation. In the first mode of operation it solves the unknown parameters of the system (positions and angles) having provided the geometry and measurements of sensing devices. This step is performed by minimising procedures. In the second mode SIMULGEO is also capable of performing the full error propagation including correlations between various sub-components linked via common mechanical supports. This step is based on the matrix operations and the analytical approach to propagation of small errors.

### Train Monte Carlo

Since the process of measurement generation and reconstruction is fully automated it is also possible to use SIMULGEO in the train Monte Carlo by solving the unknown positions of markers in many repeated “train journeys” along the tunnel varying each time the measurements. Such an approach allows to explore the full distribution of the errors under study. It provides also a tool to investigate the systematic effects in the reconstruction trying to solve the system assuming different (miscalibrated) geometry with respect to the true geometry used in the ray tracer for the generation of measurements. In addition by varying the miscalibration patterns (“deltas” of the sensing elements) one can study the distribution of systematic errors as a function of the precision of the calibration procedure.

The main steps of the algorithm of the Train Monte Carlo are following:

1. generate TRUE wall markers positions along the accelerator tunnel (nominal values smeared by  $\sigma = 10 \text{ mm}$  in  $X, Y, Z$  direction)
2. LOOP over “miscalibration patterns” for CCDs/FSI launch points and retro-reflectors on the train. Positions and angles of sensing elements are smeared by  $\sigma = 1 \mu\text{m}$  or  $1 \mu\text{rad}$ , respectively.
3. LOOP over runs (train journeys) along the tunnel for a given train
  - 3a. LOOP over cars in the train
    - generate car stops in front of wall markers (smeared by  $\sigma = 10 \text{ mm}$  ( $pos$ ),  $\sigma = 10 \text{ mrad}$  ( $ang$ ))

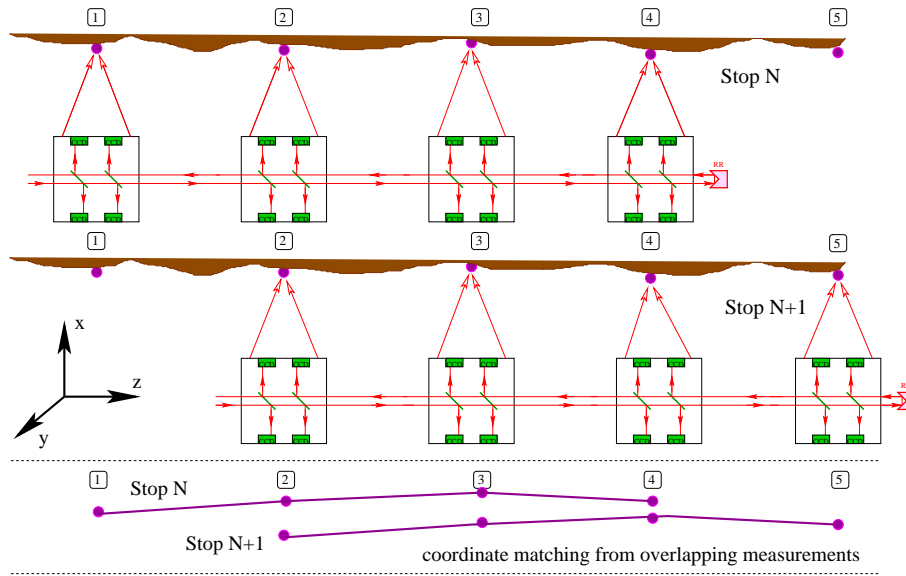


Figure 2: Principle of the LiCAS train operation. Top view of the two train stops along the accelerator tunnel are presented. For detailed description see text.

- transfer all coordinates of CCDs/FSI to the global (tunnel) frame
  - generate measurements of sensing units using Ray Tracer and TRUE geometry on input (CCDs, FSI measurements are smeared by resolution of  $\sigma = 1 \mu m$ )
4. RECONSTRUCT the system w.r.t. the unknown position/angles of cars and wall markers using MISCALIBRATED geometry and smeared measurements
  5. collect histograms, calculate statistics for RECONSTRUCTED-TRUE variables

## RESULTS OF THE TRAIN SIMULATIONS

The long-distance operation of the train inside the accelerator tunnel was simulated by a set of many identical trains displaced by  $25 m$  (distance between stops), each pair of them coupled via 3 overlapping wall markers. Figure 3 (left) contains the results obtained for the statistical error propagation over 24 train stops ( $600 m$ ). Analytical predictions given by SIMULGEO are compared to the Monte Carlo results (RMS of the RECONSTRUCTED-TRUE distribution of corresponding variables). Right plot contains example for the growth of systematic errors (MEAN value of the RECONSTRUCTED-TRUE distribution of corresponding variables) for one particular miscalibration of the train. Straight line fits used for the calculation of the RMS of the residua distribution for various “miscalibration patterns” are also shown.

The above results were obtained assuming the intrinsic resolution of the CCD cameras and FSI lines (both internal and external) equal to  $\sigma_{CCD} = \sigma_{FSI} = 1 \mu m$ . Monte Carlo simulation was performed under the assumption that

all calibration constants (positions and rotations of CCD cameras, FSI light sources and retro-reflectors) are known to the accuracy of  $\sigma_{pos} = 1 \mu m$  for positions and  $\sigma_{ang} = 1 \mu rad$  for angles.

### Random Walk Model

In order to interpret the above results a simple model of random walk has been developed. In this approach the procedure of accelerator alignment resembles the construction of a long straight line using short ruler.

For statistical uncertainties the overall error after  $n$  steps is a convolution of the precision of the ruler and the precision of the placement of the ruler with respect to the previous measurement. Taking into account the error of the positioning of the ruler and the angular error the following formulas can be derived:

$$\sigma_{x,n}^{stat} = \sqrt{l^2 \sigma_\alpha^2 \frac{n(n+1)(2n+1)}{6} + \sigma_x^2 \frac{n(n+1)}{2}} \quad (1)$$

$$\sigma_{y,n}^{stat} = \sqrt{l^2 \sigma_\beta^2 \frac{n(n+1)(2n+1)}{6} + \sigma_y^2 \frac{n(n+1)}{2}} \quad (2)$$

$$\sigma_{z,n}^{stat} = \sqrt{\sigma_z^2 \frac{n(n+1)}{2}} \quad (3)$$

where  $n$  is the wall marker number,  $l$  is the effective length of the ruler (distance between cars of  $25 m$ ), and the corresponding errors are the parameters of the random walk:  $\sigma_\alpha$ ,  $\sigma_\beta$  are the angular errors in ZX and ZY planes respectively,  $\sigma_x$ ,  $\sigma_y$  are the transverse errors and  $\sigma_z$  is the longitudinal error. From the fit to the error propagation curves obtained from the full SIMULGEO model the following values for the random walk parameters were extracted:  $\sigma_\alpha = 25.8 \pm 1.1 nrad$ ,  $\sigma_\beta = 55.4 \pm 1.9 nrad$  and  $\sigma_z = 0.15 \pm 0.02 \mu m$ . Values for  $\sigma_x$ ,  $\sigma_y$  are less than

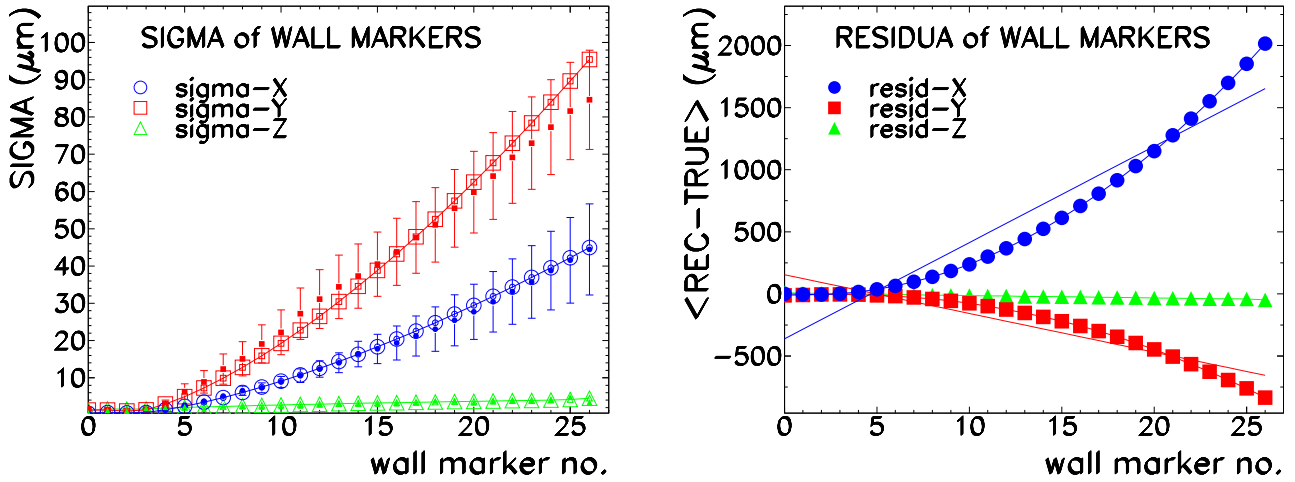


Figure 3: Errors propagation over 600  $m$  tunnel for the reference markers. Left plot contains statistical errors from the analytical SIMULGEO calculations (open points) overlaid with the Monte Carlo results (solid points). Right plot presents accumulation of systematic errors for a particular train miscalibration. Straight line fits used to calculate the RMS of the residua distribution for various “miscalibration patterns” are also shown.

5  $\mu m$  and are compatible with zero within errors. Their contribution is negligible comparing to the angular term.

The asymptotic behaviour of the above formulas is  $\sigma_{xy,n}^{stat} \sim n^{\frac{3}{2}}$ , and  $\sigma_{z,n}^{stat} \sim n$ . Fast growth of transverse errors is a consequence of the fact that the contributing errors of individual measurements are highly correlated and the precision of the  $n^{th}$  element depends on the precision of all previous points.

For systematic errors using similar “short ruler” model the following formulas were obtained:

$$\sigma_{x,n}^{syst} = l\Delta_{\alpha}n(n+1)/2 + n\Delta_x \quad (4)$$

$$\sigma_{y,n}^{syst} = l\Delta_{\beta}n(n+1)/2 + n\Delta_y \quad (5)$$

$$\sigma_{z,n}^{syst} = n\Delta_z \quad (6)$$

where  $n$  is the wall marker number,  $l$  is the effective ruler length (car-to-car distance of 25  $m$ ),  $\Delta_{\alpha}$ ,  $\Delta_{\beta}$  are the systematic angular errors in ZX and ZY planes respectively and  $\Delta_x$ ,  $\Delta_y$ ,  $\Delta_z$  are the systematic transverse and longitudinal errors. The above parameters were extracted from the fit to the curves given by the full SIMULGEO model for different “miscalibration patterns” of CCDs and internal and external FSI launch points and retroreflectors varied by Gaussian errors of 1  $\mu m$  (or 5  $\mu m$ ) for positions and 1  $\mu rad$  (or 5  $\mu rad$ ) for angles. The mean values for  $\Delta_{\alpha}$ ,  $\Delta_{\beta}$  and  $\Delta_x$ ,  $\Delta_y$ ,  $\Delta_z$  are compatible with zero within errors. Their dispersions (RMS) are summarised in table 1. Comparing to statistical errors the asymptotic behaviour of the transverse systematic errors exhibits even faster growth:  $\sigma_{xy,n}^{syst} \sim n^2$ , what strongly favours longer trains with fewer number of stops.

The obtained predictions refer to the precision of the placement of the  $n^{th}$  accelerator component with respect

Parameter	var. 1 $\mu m/1 \mu rad$	var. 5 $\mu m/5 \mu rad$
$RMS(\Delta_{\alpha})$	$1.0 \pm 0.2 \text{ nrad/m}$	$4.6 \pm 1.0 \text{ nrad/m}$
$RMS(\Delta_{\beta})$	$2.3 \pm 0.4 \text{ nrad/m}$	$10.5 \pm 2.3 \text{ nrad/m}$
$RMS(\Delta_x)$	$1.2 \pm 0.2 \mu m$	$5.3 \pm 1.2 \mu m$
$RMS(\Delta_y)$	$2.7 \pm 0.4 \mu m$	$12.1 \pm 2.7 \mu m$
$RMS(\Delta_z)$	$0.8 \pm 0.1 \mu m$	$2.9 \pm 0.6 \mu m$

Table 1: RMS of the systematic errors parameters from equations 4,5,6 obtained for two different “miscalibration patterns”. Systematic angular errors are normalised by dividing by the car-to-car distance of 25  $m$ .

to the first one. However, this is not the ultimate measure of the quality of the accelerator alignment. The relevant parameter is the mean deviation of each component from the ideal straight line which can be expected from the above procedure. To obtain the final prediction on the statistical deviation of the alignment from the straight line a series of random walk trajectories was generated using the parameters fitted to the SIMULGEO points (fig. 4). A straight line was fitted to each trajectory and the corresponding residua were calculated. The extracted RMS values of the residua distributions (fig. 5) for each marker along 600  $m$  provide the measure of the statistical accuracy of the whole procedure. Because of high correlation between errors for  $n$  and  $n+1$  marker the generated trajectories exhibit much smaller oscillations that would be expected from completely random process. Interesting feature of our model is the fact that X errors are smaller than Y errors. This is because of the higher sensitivity of Y errors to the car rotation around Z axis which does not influence so much X coordinate (where the precision is mainly dominated by the FSI distance measurements). It is worth to stress out that the precision for X – Y position recon-

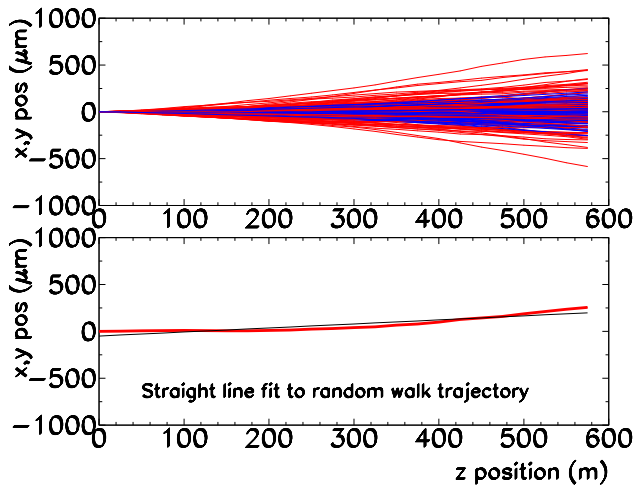


Figure 4: Examples of the random walk trajectories (upper plot) and straight line fit to selected trajectory (lower plot).

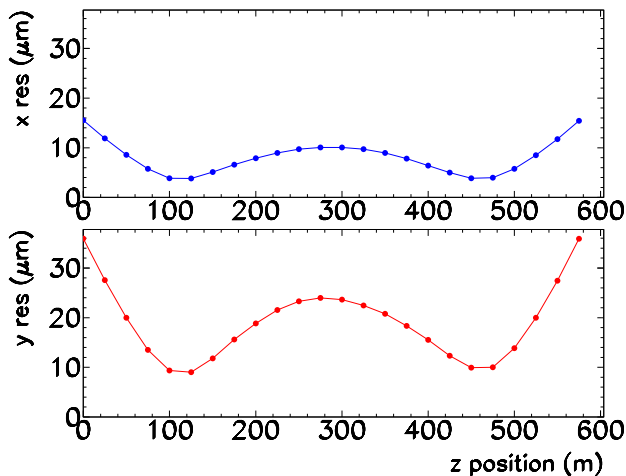


Figure 5: RMS of residua distributions from straight line fit to the random walk trajectories (ie. statistical errors only): upper plot horizontal (X) errors, lower plot vertical (Y) errors.

struction can be swapped by changing the position of the wall marker from horizontal to vertical location or by placing two wall markers in front of each LiCAS car. Similar procedure was applied to the parabola curves describing the growth of systematic errors (see fig. 3 right). The RMS of the residua distributions for different train miscalibrations are presented in figures 6 and 7.

Figure 6 describes the optimistic scenario with the calibration constants determined to the level of  $1 \mu m$  (positions) and  $1 \mu rad$  (angles) while figure 7 was obtained under the assumption that the calibration constants are known to the level of  $5 \mu m$  and  $5 \mu rad$ , respectively. It provides the measure of the size of safe margin at which the specification of the vertical alignment of  $200 \mu m$  over  $600 m$  is

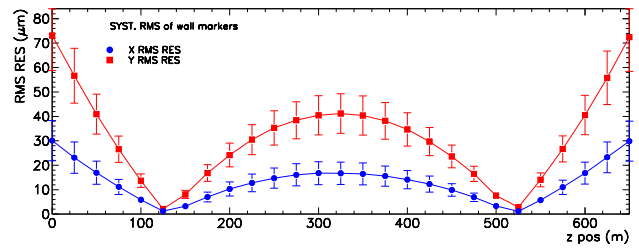


Figure 6: RMS of residua distributions from straight line fit to the parabolic trajectories (ie. systematic errors only) assuming miscalibration of  $1 \mu m$  (positions) and  $1 \mu rad$  (angles).

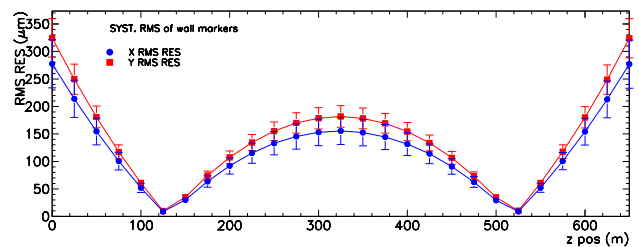


Figure 7: RMS of residua distributions from straight line fit to the parabolic trajectories (ie. systematic errors only) assuming miscalibration of  $5 \mu m$  (positions) and  $5 \mu rad$  (angles).

reached.

## REFERENCES

- [1] P.A. Coe, D.F. Howell and R.B. Nickerson, "Frequency scanning interferometry in ATLAS: remote, multiple, simultaneous and precise distance measurements in a hostile environment", Meas. Sci. Technol. 15 (2004) 2175-2187.
- [2] A.F. Fox-Murphy et al., "Frequency scanned interferometry (FSI): the basis of the survey system for ATLAS using fast automated remote interferometry", Nuclear Instruments and Methods in Physics Research A 383 (1996) 229-237.
- [3] A. Reichold et al., "The LiCAS Rapid Tunnel Reference Surveyor. The status after commissioning", IWAA-2008, published in this Volume.
- [4] "First measurements from the Laser Straightness Monitor of the LiCAS Rapid Tunnel Reference Surveyor", IWAA-2008, published in this Volume.
- [5] "Calibration Of The LiCAS Reference Interferometers", IWAA-2008, published in this Volume.
- [6] L. Brunel, "SIMULGEO: Simulation and reconstruction software for optogeometrical systems", CERN CMS Note 1998/079.